Method Development to Process Hyper-Temporal Remote Sensing (RS) Images for Change Mapping

Jose Maria Beltran-Abaunza

March, 2009

Course Title:	Geo-Information Science and Earth Observation for Environmental Modelling and Management
Level:	Master of Science (Msc)
Course Duration:	September 2007 - March 2009
Consortium partners:	University of Southampton (UK) Lund University (Sweden) University of Warsaw (Poland) International Institute for Geo-Information Science and Earth Observation (ITC) (The Netherlands)
GEM thesis number:	2007-03

Method Development to Process Hyper-Temporal Remote Sensing (RS) Images for Change Mapping

by

Jose Maria Beltran-Abaunza

Thesis submitted to the International Institute for Geo-information Science and Earth Observation in partial fulfilment of the requirements for the degree of Master of Science in Geo-information Science and Earth Observation for Environmental Modelling and Management

Thesis Assessment Board

Prof. Dr. Ir. E.M.A. Smaling (Chair)
Dr. Dr. A.G. Toxopeus (Internal examiner)
Prof. Dr. hab. Katarzyna Dąbrowska-Zielińska (University of Warsaw, external examiner)
Dr. Ir. C.A.J.M. de Bie (Supervisor)

ITC International Institute for Geo-Information Science and Earth Observation
Enschede, The Netherlands

Disclaimer

2+1º
3OFH

"El mundo está en las manos de aquellos que tienen el coraje de soñar y correr el riesgo de vivir sus sueños".
Paolo Coelho

Abstract

This research showed that by using a modified version of the adaptive Savitzky-Golay filter to force an upper envelope to a noisy NDVI time-series, it is possible to reduce noise, and obtain images that are representative of the good original NDVI values. Following the removal of periods of high variability (due to snow), from an NDVI noise-reduced time-series, it is possible to detect individual years within a class that are significantly different from yearly averaged values of the class. This is the first indication of classes with tendency of changes. By using a formulated Key Index in this research, based on the averaged years within a class, pairs of classes surpassing a Key Index threshold can be merged. This method takes into account of inter-annual variability. Furthermore, the method produced a temporal reference library, with a unique legend of signatures that could be used for change mapping studies.

Acknowledgements

Supported by the Programme Alβan, the European Union Programme of High Level Scholarships for Latin America, Scholarship No. E07M400482MX.

My most sincere thanks to the staff of the EU Erasmus Mundus Consortium (University of Southampton, UK; University of Lund, Sweden; Warsaw University, Poland and ITC, The Netherlands) that runs such an exceptional graduate programme, the experience has truly been one of the best.

To Wim Bakker, my python guru.

To my supervisor Kees de Bie, it has been my pleasure to learn from you. Thank you for all your advice and strong sense of direction.

To my family that supported my adventure.

To my wife Marcela, and my daughter Ana Sofia, my endless sources of love, inspiration, fun and commitment.

To all my friends around the world, thank you all!

Table of contents

List of figures

List of tables

1. Introduction

1.1. Monitoring ecosystems

The increase of human activities have led to degraded habitats and reduced ecosystem services (Kerr and Ostrovsky, 2003). Human pressures will continue to meet future demands for food, water and shelter (UNEP, 2007). The global priority to protect ecosystems requires indicators to monitor the present-day ecosystem change. This can provide e.g. more proof in attributing observed climate change phenomena to anthropogenic causes (Bates et al., 2008).

Land cover, the ground feature on earth that serve as the observed backdrop of biophysical settings (Jones et al., 1997), expresses the dynamics of ecosystems due to climatic, hydrologic, geographic or human influences. Observed changes consist of land surface transformations or conversions (Bontemps et al., 2008; Lambin and Linderman, 2006) and due to the fact that land cover is captured by recorded Electro Magnetic Radiation (EMR) of satellite images (de Bie et al., 2000) several Remote Sensing (RS)-based methodologies and techniques have been in use to extract, observe and interpret changes that influences ecosystem functions (Lu et al., 2004).

Detecting and monitoring changes that relate to ecosystem processes are still not fully quantified or understood (Bates et al., 2008). It requires among others the integration of spatial and temporal aspects (Beck et al., 2008) where RS data with more than 30 years of imagery available (Zhou et al., 2008), play a key role as data source of spatial and temporal information (Schmidt and Skidmore, 2003).

The spatial heterogeneity of the combination of physical and biological factors that drive ecosystem processes (Guo et al., 2003), can be reflected in the phenological patterns of vegetation (de Bie, 2002; de Bie et al., 2008). Those patterns can be represented by vegetation indices (Pettorelli et al., 2005) and its spatial and temporal variability can be recorded. Therefore the response of vegetation to its environment as measured by vegetation indices can be used to monitor environmental quality and land cover change (Cleland et al., 2007; Fung and Siu, 2000; Pettorelli et al., 2005).

RS-based vegetation indices are mainly derived from the absorption of red radiation by pigments like chlorophyll and scattering of Near-Infra-Red (NIR) radiation by foliage (Beck et al., 2006) and are good indicators of chlorophyll activity (Pettorelli et al., 2005). By using a Bray Curtis normalization over the reflectance ratio of these portion of the electromagnetic spectrum (see Equation 1), the Normalized Difference Vegetation Index (NDVI) arises (Chen et al., 2004).

Equation 1. Normalized Difference Vegetation Index

$$NDVI = \frac{NIR - R}{NIR + R}$$

Where:
NIR → Near Infrared Band
R → Red band

The NDVI is being the most widely used vegetation index (Pettorelli et al., 2005). It is used to study the spatial and temporal trends in vegetation dynamics, productivity and distribution (Beck et al., 2008; Kerr and Ostrovsky, 2003; Nemani and Running, 1997; Pettorelli et al., 2005).

Correct use of the large collection of satellite data involves assumptions that should not be ignored or overlooked. They are summarized by Duggin and Robinove (1990). Care should be taken when using NDVI time-series; noise remaining after applying atmospheric corrections, could still remain, like noise derived from clouds or aerosols (Hird and McDermid, 2009). This results in a decrease of the NIR radiance due to reduction of atmospheric transmission, and at the same time, an increase in the red radiance by additive path radiance. In turn this results in a lower signal recorded at the Top-of-Atmosphere (TOP) when compared with the signal recorded at the Top-of-Canopy (TOP), so the NDVI is then negatively biased (Beck et al., 2006).
Furthermore, Bradley et al., (2007) mention the limitation of using NDVI-based phenology to detect change due to noisy NDVI datasets. Hird and McDermid (2009) mention: "*the negative bias caused by unfavourable conditions and anisotropic bidirectional effects are a prevalent and well-recognized feature of a noise NDVI data sets*."
Methods have been developed to reduce the contamination of NDVI time-series by clouds or atmospheric variability (Beck et al., 2006; Bradley et al., 2007; Chen et al., 2004; Hermance, 2007; Hermance et al., 2007; Jönsson and Eklundh, 2002; Jönsson and Eklundh, 2004). Although, Hird and McDermid (2009) mention that: "*there is a strong need for a more comprehensive understanding regarding noise reduction on these datasets*."

1.2. Research Problem

In order to manage the ecosystem services efficiently and wisely, it is required to advance our understanding of the processes behind the observed natural patterns (Nogues-Bravo et al., 2008) and increase our ability to map changes. Detecting change requires a unique legend that is able to represent the features of interest amongst the processed spatial-temporal resolution of the images used (de Bie, 2008; personal communication).

Although great efforts have been done to provide accurate methods to classify and detect change, none of these have used fully the rich information of hyper-temporal images to develop a legend based on the data itself, and then, to detect change before being the feature or object with the reality.

This research aims to develop a methodology building on de Bie et al. (2008); de Bie and Nidumolu (2004) to derive a unique spectral library is derived using only the information of the hyper-temporal images used. NDVI time series without being previously related to any object in reality can in theory, be used to derive a spectral library from the data itself, if features and their changes indeed captured by the NDVI images used.

2. Research Objectives

A summary of the research objectives is shown in Figure 1.

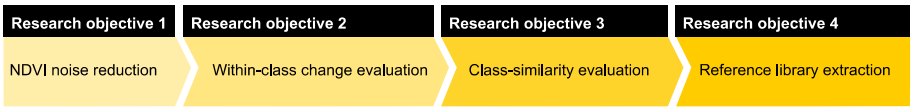

Figure 1. Main processes involved in this research.

2.1.1. Study Objective

To develop a methodology using hyper-temporal images to produce a unique legend derived from the data itself before being related with actual objects or features in the reality and which can be used to create RS-based change maps.

2.1.2. Research Questions and Hypotheses

Research question 1

How to perform a noise reduction technique and fill-in missing data over a stack of hyper-temporal NDVI-SPOT-VGT-S10 covering the period of April 98 –April 08 (10 years period) for Poland while enhancing the real information present.

Hypothesis

Ho: A streaming film of sequential images fluctuates around 'good' original values.
Ha: A streaming film of sequential images is smooth and without shocks and are representative for the good original values.

Research question 2

How to evaluate by class, if within the 10 years period change occurs? This research question will follow an iterative process of unsupervised classification of the images through the ISODATA clustering technique.

Hypothesis

Ho: Individual years within a class are not significantly different from the yearly averaged values of the class.
Ha: Individual years within a class are significantly different from the yearly averaged values of the class.

Research question 3

How can similarity between signatures be evaluated? This aims to merge classes that differ regarding inter-annual variability but that are similar in behaviour when averaged over years.

Hypothesis

Ho: Two classes (to be defined later) are similar if a threshold of similarity index (KI) is surpassed (KI >=0.7).
Ha: Two classes (to be defined later) are dissimilar if a threshold of similarity index (KI) is surpassed (KI >=0.7).

2.1.2.1. Research question 4

How to extract unique annual profiles and express the signature library in a data file as required to mapping changes?

3. Methodology

3.1. Study area

The study area refers to the territory of Poland (see Figure 2) covering an area of 312,679 km^2 in Western Europe (Central Statistical Office, 2008).

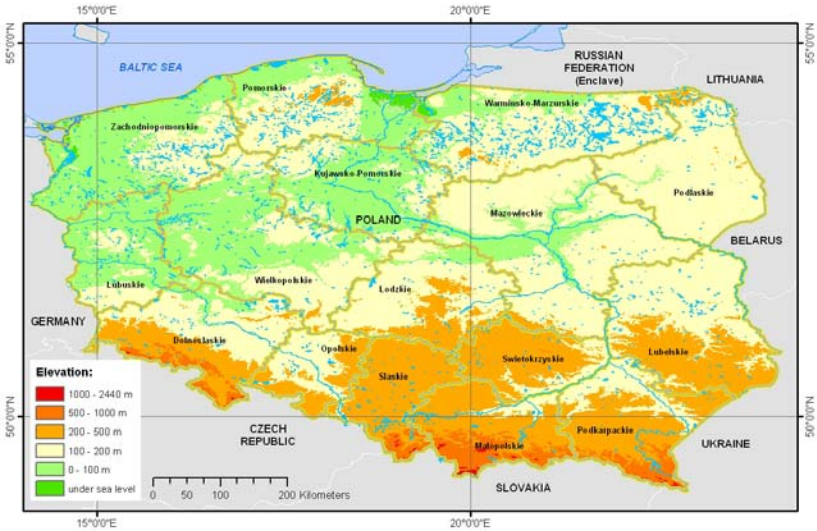

Figure 2. Study area showing the current 16 Voivoidships (Districts) boundaries in Poland and main altitudinal ranges.

The topography of Poland is dominated by low elevation areas that stretch from France to Ukraine creating wind corridors for humid air masses that move quickly from the Atlantic or North Sea towards East and that collide above Poland with dry air coming from the Eurasian interior. As a result the weather tends to have substantial changes in consecutive years with hot and dry summers that have cold and wet periods. In general, summer precipitation tends to be 2-3 times higher than in winter. A visible effect of Poland's highly variable weather is that the sky overcast cloudiness is 60-70% in a year (Poland Gateway, 2006). This caused that of the used de-cloudy hyper-temporal image series became a requirement.

3.2. Data used

Composite NDVI images derived from SPOT-4 & SPOT 5 VEGETATION 10-day synthesis (VGT-S10) at 1-km2 resolution were chosen among other sensor and satellite platforms because they have up to date, the best balance on spatial and temporal resolutions (1km^2 spatial resolution with a swath width of 2,250 km, time-series starting at 1998 to the present and are freely available). The VEGETATION (VGT) instrument on-board the satellite is a wide field of view sensor which operates in four spectral bands (see Table 1).

The hyper-temporal stack used for the research contains 360 geo-referenced de-clouded* composite NDVI images recorded between April 01, 1998 and up to March 31, 2008 (covering a period of 10 years) for Poland. These images were obtained from www.vgt.vito.be.

Table 1. Range of operation of the spectral bands available on the VEGETATION instrument.

Spectral band	Wavelength
B0 (Blue)	**0.43 - 0.47 µm**
B2 (Red)	**0.61 - 0.68 µm**
B3 (Near Infrared-NIR)	**0.78 - 0.89 µm**
Middle Infrared/Short Wave Infrared (MIR/SWIR)	**1.58 - 1.75 µm**

Source: VEGETATION Program. Available from: http://www.spot-vegetation.com/

Each image is generated by using the best quality† daily image values over a 10-day period which is denoted by the number 01, 11 and 21 which refers to their respective 10-day period: 1-10, 11-20 and 21-30 days of each month (VEGETATION Program Available from http://www.spot-vegetation.com/ [Accessed on: February 2009].

* According to Skidmore et al.,(2006) the word *de-clouded* means: "*using by image and pixel of the mosaic, based on the additionally supplied quality records, only pixels that satisfy certain quality requirements* "; de Bie (personal communication, February 2009) added to this: "*These requirements are 'good' radiometric quality for bands B2 and B3 that the pixels were not labelled as 'shadow', 'cloud' or 'uncertain' but as 'clear' (removed pixels were flagged as 'missing')*".

† Refer to the products format definition section (status map plane) in the user guide of the VGT products for complete description about quality records. Available online from: http://www.spot-vegetation.com/ [Accessed: February 2009].

All the images of this period are compared pixel by pixel to pick out the 'highest' NDVI value-'maximum value at Top of Atmosphere-TOA' (de Bie, 2008; personal communication).

The NDVI is converted to a digital number (DN-value) in the 0-255 data range using Equation 2 (de Bie, 2008; personal communication) to facilitate computations and to reduce the memory needs to store the images. The bad-quality pixels that were flagged during the de-clouded process were set to 0.

Equation 2. Scaled NDVI

$$DN = \frac{NDVI + 0.1}{0.004}$$

Table 2. Sources of data used.

Source	Dataset	Available from
VEGETATION Program	VGT-S10 covering the period 01-04-1998 up to 31-03-2008 [10 years period]	www.vgt.vito.be.
European Environment Agency	Corine land cover changes (CLC1990 - CLC2000) 100 m - version 9/2007 (.Tiff)	http://dataservice.eea.europa.eu/

3.3. Software used

The software and its category of application are presented in Table 3**.**

Table 3. Software used in this research

Application	Software	Modules or extensions
Image processing	Leica Geosystems ERDAS Imaging v9.2	Classification
Image processing	RSI ENVI 4.5	Spectral Library Builder
Image visualization	GEM Viewer[‡] 0.8	
GIS[§] spatial analysis	ESRI ArcGIS 9.3: ArcInfo	Spatial analyst extension
Statistics	SPSS 16.0	Non-parametric tests
Programming	Python 2.5	SCIPY[**], GDAL[††], GEM Tools [‡‡]

[‡] GEM viewer is an open source-python based application (alpha version) able to visualize the hyper-temporal images and plot their yearly temporal profiles, standard deviation and mean profiles by class. It can spatially visualize the image time series and mask the occurrence of a particular class; developed by this author in 2008.

[§] Geographic Information System - GIS

[**] Scientific tools for Python – SCIPY. Available from: http://www.scipy.org/SciPy

[††] Geospatial Data Abstraction Library - GDAL. Available from: http://www.gdal.org/

[‡‡] GEM Tools is a python based-alpha version of a set of tools for image processing and visualization, developed by this author in 2008.

3.4. Method

A summary of the methodology is described in Figure 3.

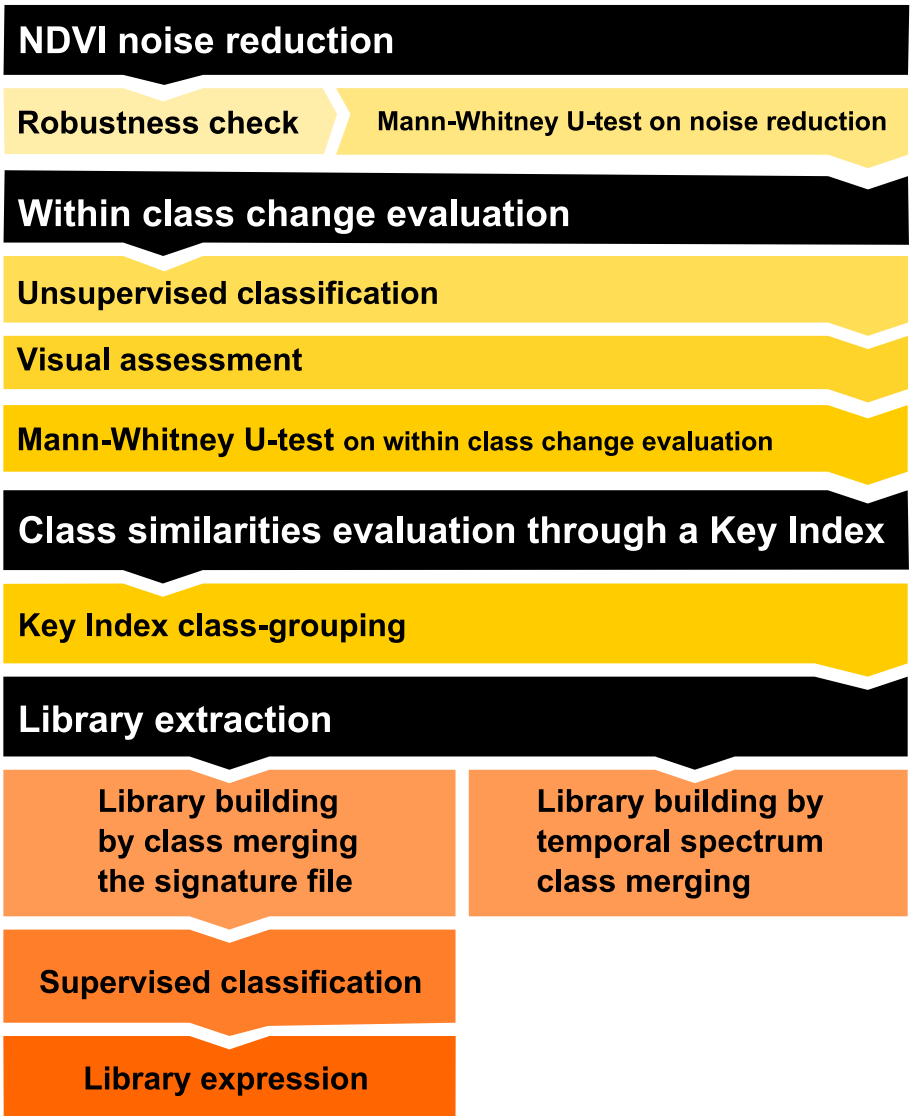

Figure 3. Methodology flow chart.

3.4.1. NDVI noise reduction

A modification of the Adaptive Savitzky-Golay filter (ASAVGOL) algorithm built in TIMESAT 2.3– a Program for Analysing Time-Series of Satellite Sensor Data (Jönsson and Eklundh, 2004) was used to force an upper envelope and to reduce the noise in the hyper-temporal NDVI stack.

The Savitzky Golay filter (SAVGOL) uses a simplified least squares procedure to smooth and differentiate data (Savitzky and Golay, 1964) by suppressing disturbances and replacing each data value by a linear combination of nearby values in a time window (Jönsson and Eklundh, 2004).

The main difference between the common SAVGOL and ASAVGOL is that in the latter, the fitting allows iterations. The width of the moving window that determines the degree of smoothing was initially set by the user and then, at later iterations, the algorithm takes control to capture the corresponding sudden increase or decrease of the underlying data values (Jönsson and Eklundh, 2004).

Each image in the stack had a vegetation index value, $\boldsymbol{y}$, which creates an array at specified time $\boldsymbol{t}$. Thus, the times-series ($\boldsymbol{t_i}$, $\boldsymbol{y_i}$) is built through extraction of values at pixel ($\boldsymbol{j}$, $\boldsymbol{k}$), where $\boldsymbol{i}$ represents individual images in the stack (i= 1,2,…, N). The algorithm can include a weighting system ($\boldsymbol{w_i}$) based on ancillary data (like in ASAVGOL), such as cloud indicators, to mark outliers.

After iteration of test and adjustments, in this research, the algorithm[§§] was run with 4 iterations with initial window sizes of 1, 2, 3 and 4 respectively, from both the left- and right-hand neighbours of the $\boldsymbol{t}$ corresponding value.

A function for spike detection identifies outliers in the hyper-temporal stack where, "values that are substantially different from both the left- and right-hand neighbours and from the median in the current time-window size are classified as outliers and are assigned weight 0" (Jönsson and Eklundh, 2004). A zero weight value (w = 0) was then assigned to flagged values (from de-clouded data), and the rest were assigned w = 1.

[§§] Refer to Jönsson and Eklundh (2004) for a complete description of the functions used in the TIMESAT v2.3 and the implementation of the ASAVGOL filter. The implementation of the modified version of ASAVGOL used in this study can be found in appendix 8.1.

The iterations used in ASAVGOL, results in a model function that is adapted to the upper envelope of the data; where data points below the model function after the first iteration are considered as being less important, and from the second iteration the system is solved using the weights. For each new iteration, the filtering is calculated with the new locally adapted size of the window and with the new values of the model function. The multi-step fitting process can continue until some sort of self-consistency is obtained (Jönsson and Eklundh, 2004).

The core modification made to ASAVGOL filter in this study was that during the iterations if the fitted value resulted to be less than the actual value and have a weight different from 0, the algorithm forces to use the original value instead of the calculated by the function. The size of the time window, self-adjust for successive iterations, using the initial sizes defined at the beginning of the iterative process. This ensures that the model function follows the highest values in the data whilst performing the smoothing to enhance the real information present.

Robustness check

Mann-Whitney U-test on noise reduction

The Mann-Whitney U-test is a non-parametric test similar to the Students t-test (MacFarland, 1998). The Mann-Whitney U-test was selected because it allows two-independent sets of measurements with no restriction about its distribution to be tested for the null hypothesis that both sets belong to the same populations (Kruskal and Wallis, 1952; Milton, 1964). If the calculated two tails p-value is less than the significance level then the difference is not just the result of random noise and the two sets of measurements are said to be genuinely different (MacFarland, 1998).

The Mann-Whitney was used to test the two algorithms of NDVI noise reduction, ASAVGOL and the Modified version of ASAVGOL (MASAVGOL). A random pixel (row 610, column 197) was selected from the NDVI stack and its temporal profile was extracted. The latter was filtered using both algorithms. The robustness of MASAVGOL was checked by running the non-parametric Mann-Whitney-U-test using the software SPSS with a significance level of 0.05, against the model ASAVGOL that is built in TIMESAT 2.3 (Jönsson and Eklundh, 2004).
Literature recommends to use Mann-Whitney when the number of elements in each set is equal or less than 20 (Milton, 1964). Thus both, the ASAVGOL and MASAVGOL, were checked against each other 18 times by taking 20 consecutive elements at a time.

3.4.2. Within class change evaluation

Unsupervised classification

The unsupervised classification is a clustering method, where objects are characterized as patterns or points in a *d*-dimensional space. The clustering is based on the proximity of similar objects. The proximity of the objects could be the distance between pair of points, and through the proximity matrix the algorithm performs the classification with no a-priority partitions of the objects being used (Jain and Dubes, 1988). The resulting cluster labels require expert guidance (supervised classification) in order to relate objects with reality (de Bie; personal communication, September 2008).

The unsupervised clustering scheme used in the research was the Iterative Self-Organizing Data Analysis Technique (ISODATA). The ISODATA is one of the most widely used clustering algorithms (Memarsadeghi et al., 2003). It calculates the spectral distance and iteratively classifies the pixels until a minimum spectral distance is achieved (Tou and Gonzalez, 1974).

The spectral distance is the angle between two spectral vectors, $\vec{v}$ and $\vec{w}$. Can be calculated using the dot product $\vec{v} \cdot \vec{w}$ from the Equation 3 (Bakker and Schmidt, 2002).

$$SA(\vec{v}, \vec{w}) = \cos^{-1}\left(\frac{\vec{v} \cdot \vec{w}}{\|\vec{v}\| \|\vec{w}\|} \right)$$ Equation 3. Spectral angle.

The ISODATA algorithm was applied to the cleaned NDVI stack using ERDAS imaging 9.3 with a maximum number of iterations of 35 and the convergence threshold was set to 1.0. The unsupervised classification was then run 85 times to define 10 to 95 unsupervised classes, an to obtain respective 85 signature files. Using the function of divergence statistics by signature file in ERDAS imaging, the values of average and minimum separability were obtained.

A heuristic visual approach is used to identify the optimal number of classes to use for the unsupervised classification. Generally, when an evident and coincident peak in the average and minimum separability profiles is found in the graph, the related number of classes is selected as optimal, otherwise the researcher should try to keep the number of classes small while the separability stats must be high ‘smaller peaks’ (de Bie; 2008, personal communication).

Within class change assessment

The derived signature file contains the information about the classified clusters in the NDVI stack. By class, the mean values for each point in the time-series were exported as a text file, using the ERDAS imaging signature editor.
The exported file has all the class related information in one row. The file was re-arranged to facilitate the evaluation of the class variability by moving yearly column values by class in a separate row. The within class variability was assessed, visually and statistically by means of the Mann-Whitney U-test with a confidence level of 0.05.

Visual assessment

A gradual colour change was assigned to each curve from year 1 to year 10. All curves for a particular class were plotted together using this colour scheme. The visual method tries to find if there is a pattern of change over the years. A slightly change in colours defines the pattern (see Figure 4).

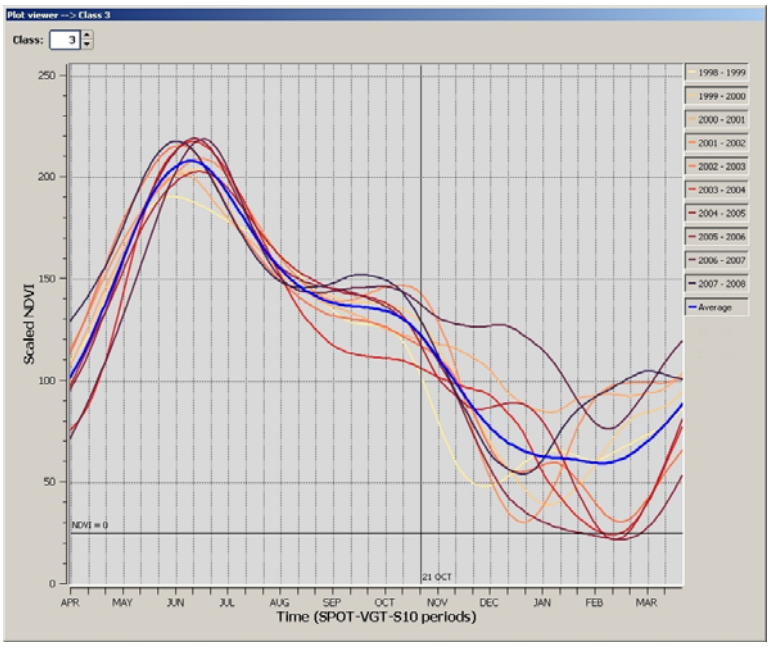

Figure 4. Example of the colour scheme used to evaluate within class change.
The black vertical line- Oct 21 defines the last value in the time series with relatively low variability compared with the high variability of the following winter period. The horizontal black line defines the NDVI = 0 limit (when is not scaled).

Statistical assessment using Mann-Whitney U-test

As an aid of the visual interpretation each curve in the class was tested for similarities against the mean value of the curves. A Mann-Whitney U-test was then run with a significance level of 0.05. Only the first 20 of 36 values of the profile were used for testing the significance. These values represent the period from April 01 up to October 31. The remaining points covering the winter period were excluded from this part of the analysis due to high variability in snowy conditions that generally are present in Poland during this time of the year (Poland Gateway, 2006). They may bias the result due to high variability across years.

Years, that were not significantly different from the mean values of the class, were averaged using the 36 values of the curves which results in one mean-year with 36 values (each value represents one SPOT-VGT-S10 period) for each class. These averaged values 'temporal spectrum' were the basis of the reference library.

Anomalous years that were significantly different to mean values of the class, were removed prior to the calculation of the new mean and standard deviation values of the class.

3.4.3. Class similarities evaluation through a Key Index

To account for the similarities between averaged annual profiles of individual classes, a new index was developed. The new Key Index (KI) aimed to provide a weighting method to weight each point of the curve using its standard deviation. The curves are created around the averaged values within a class. Higher weights are assigned to points that have lower standard deviation. The latter maximises the value of the point against other points where the variability is higher.

If two curves are to be tested for similarities, it is expected that the line defined in each curve between the lower and upper limits of the standard deviation[***] at each point, will intersect. The length of the intersection measures the similarity between classes for each point, but it requires to be weighted first to account for its contribution to the 36 data points covering the year. It is more likely to find intersections where the variability is higher and the opposite occurs where points are found to have lower variability. Thus, points with higher variability should be weighted lower, whereas those with low variability should be weighted higher. The visualization of the concept is shown in Figure 5.

[***] See the full derivation of the Key Index on the next page.

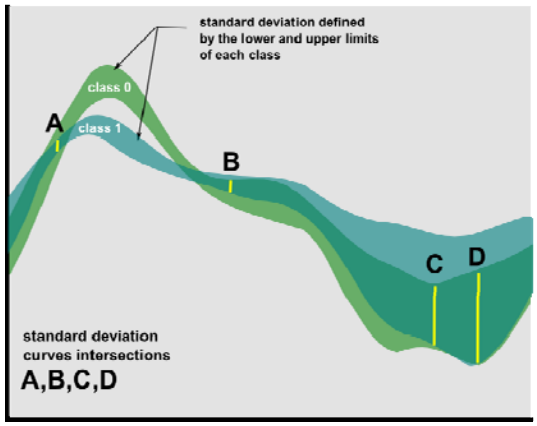

Figure 5. Fictional example showing 4 intersections over the upper and lower standard deviation curves for two unsupervised class-curves.
Points A and B have the same intersection length, but in point B the standard deviation is higher in both curves. Thus the value in B should be weighted lower than A. The same principle occurs in points C and D. Point D shows a greater length and could mislead the interpreter by observing that it is more similar the point D than C; which is incorrect. Due to the larger variation observed in point C, this point should be weighted lower than C.

The *KI* was calculated as follows:

Let $\vec{v}$ and $\vec{w}$, be the yearly averaged vectors of classes, *v* and *w*; with *n* points in time (*n*=36 for SPOT-VGT-S10 products) with corresponding standard deviation vectors, $\vec{\sigma}_v$ and $\vec{\sigma}_w$. The upper and lower point limits of the standard deviation were calculated as follows:

v-upper limit: $\vec{u}_v = \vec{v} + \vec{\sigma}_v$, v-lower limit: $\vec{l}_v = \vec{v} - \vec{\sigma}_v$

w-upper limit: $\vec{u}_w = \vec{w} + \vec{\sigma}_w$, w-lower limit: $\vec{l}_w = \vec{w} - \vec{\sigma}_w$

line distances (*d*) at each point from the upper and lower limits are calculated:

$\vec{d}_v = \vec{u}_v - \vec{l}_v$, and $\vec{d}_w = \vec{u}_w - \vec{l}_w$

Overlaps are calculated using,

$$\vec{o} = if\ \left(\max\left(\vec{l}_v, \vec{l}_w\right) < \min\left(\vec{u}_v, \vec{u}_w\right)\right) then \left(\min\left(\vec{u}_v, \vec{u}_w\right) - \max\left(\vec{l}_v, \vec{l}_w\right)\right) else\, 0$$

Half-values, *h*, on lines distances are then used to calculate the inverse of the Euclidian Distances as a weighting measure, *w*, of the overlaps,

$$\vec{h}_v = \frac{\vec{d}_v}{2}, \text{ and } \vec{h}_w = \frac{\vec{d}_w}{2},$$

$$\vec{w} = \frac{1}{\sqrt{\vec{h}_v^{\,2} + \vec{h}_w^{\,2}}},$$

the resulting weighted overlaps , *W*, are:

$$\vec{W} = \left(\vec{w}\right)\left(\vec{o}\right)^2$$

Finally, the Key Index, KI, is calculated:

$$KI = \frac{1}{2n}\sum_{1}^{n}\vec{W}$$

The KI ranges from 0 to 1. A value of 1 represents pair of classes that are completely similar and 0 the opposite.

Key Index class-grouping

The Upper-diagonal of a Cross-tabulated Table (UCT) was used to populate the KI index among all the possible combinations of classes.
The frequencies of the values in the UCT were used to estimate the threshold value for class grouping. Groups were then built. Classes having greater or equal value to the threshold value were labelled as a target for grouping.

Moving by column and row, target values were grouped together if they were sharing either a row or a column.
The threshold used in the research was a KI => 0.7 (percentage of all possible combinations).

3.4.4. Library extraction

Option 1.

Library building by class merging the signature file

The signature editor in ERDAS Imaging 9.2 was used to merge the signature of classes that in the previous KI class-grouping were identified as being similar. The original signature file with 87 classes was the source used to merge the classes. Identified anomalous years within a class were included back before merging. The new signature file became the unique signature library containing 75 classes. Note that this signature file contains the 360 values for each class.

Supervised classification

The signature library with 75 classes was linked to the cleaned NDVI stack. Using ERDAS imaging 9.2, a supervised Maximum Likelihood Classification was applied and the final classified image was generated.

Library expression

The expression of the library was made by combining the supervised classification with the CORINE Land Cover 2000 (CLC2000). A cross-tabulated table was generated using MS Access.

Using the supervised image, a map was produced by relating the corresponding level 2 classes of CLC2000.

Option 2.

Library building by temporal spectrum-class merging

The signature values derived from the KI class-grouping were averaged and a new spectrum was derived for each group. Note that the new spectrum contains only the averaged data of the years that were found to be similar to the yearly-average of the class forming the groups.

The anomalous years (anomalous spectra) derived from the assessment of within class change were treated as representatives of new classes. The anomalous spectra may repeat the cycle and check if there is any difference among the anomalous years and the mean of the anomalies for that class. The cycle finish when there is a unique set of anomalous spectrums.

This study assumed the uniqueness of the anomalous spectra and no iteration were carried out.

It is important to have an adequate labelling method to apply over the temporal spectra to build the library in such a way that the ancestors of the spectrum can be tracked back.

In this study we use 5 categories to track back the spectrum:

- Spectrum with no change (all years similar to the yearly-average of the class and not flagged by the KI-grouping), were named CLASS000_*cc*; where *cc* represent the two digits of the class enumeration.
- Spectrum with no change derived after KI class-grouping (similar to the yearly-average of the class) followed two conditions, if only two classes were merged was named MERGED*cccc,* where *cccc* represent the two digits of each class involved; if more than two classes were merged together then MMERGE*cccc* was used. The suffix *cccc* starts with the lower two digits of each class number and ends with the last two digits of the merged classes.
- Anomalous spectrum was labelled ANOMA*cc_yy*, where *cc* represent the two digits of the class enumeration and *yy* the two digits that represent the year.
- An auxiliary label with naming convention of MASKED0_00 was used to track the image-null or -zero values.

Library building

Each spectrum was exported to a text file. The structure of the file is: column 1 the index of the value representing the SPOT-VGT-S10 periods; column 2 has the values of the temporal spectrum. The file was named using the naming convention described before.

The individual files were converted to a signature library using the spectral library builder found in the spectral library tools of ENVI 4.5.

Note that the produced library (reference library) had the temporal profiles after KI class grouping plus the anomalous profiles, and the number of values on each spectrum is 36.

4. Results

4.1.1. NDVI noise reduction

Mann-Whitney U-test on noise reduction

One random pixel (row 610, column 197) was used to test the robustness of the Modified version of the ASAVGOL (MASAVGOL, see algorithm implementation in appendix 8.1) against ASAVGOL- a proven algorithm built in TIMESAT 2.3 (Jönsson and Eklundh, 2002; Jönsson and Eklundh, 2004) for reducing NDVI noise.

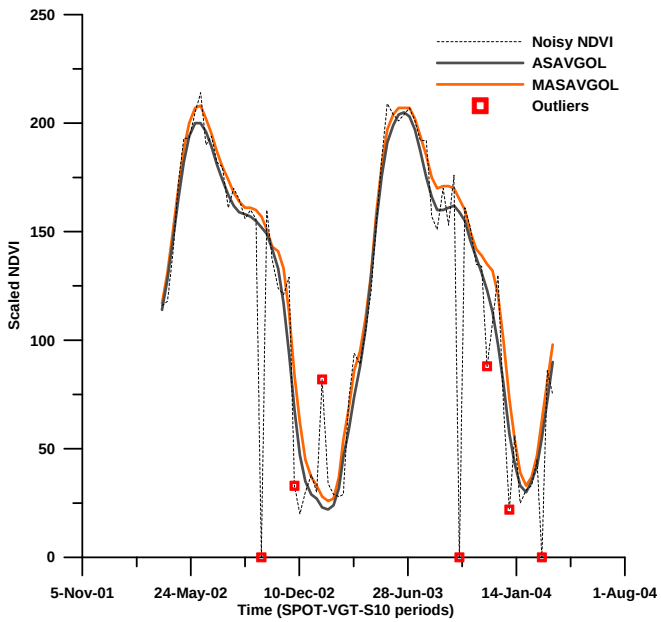

Figure 6. ASAVGOL vs. modified ASAVGOL fitted curves (two year period slice of the NDVI stack at random pixel location-(row: 610, column: 197)). The temporal window sizes used were [1,2,3,4], with all but the last iteration with an upper envelope forced.

Figure 6, shows one complete cycle in the time-series of the final output after adjusting the initial window sizes of the fitting algorithm. The red rectangles showed the location of point values that were flagged as spikes by the spike function in the algorithm. Both curves follows almost same distribution, but the profile of MASAVGOL adjusted higher to the upper envelope.

The values of the selected pixel are distributed into 360 points over the time- series. The robustness of the model used was done by checking the algorithms against each other using a Mann-Whitney U-test. Thus, to overcome the limitation on the use of the Mann-Whitney for two independent variables with more than 20 elements, the profile was segmented into smaller sections of 20 elements each, and then a Mann-Whitney U-test was applied to each section. The calculated two-tailed p-values for the 18 sections are shown in Table 4. Using a significance level of 0.05, only 1 period out of 18, were found to be different and highlighted in gray on the table.

Table 4. ASAVGOL vs. MASAVGOL Mann-Whitney U-test calculated two-tailed p-values for testing robustness of the models.

Section	SPOT VGT S10 period	Calculated significance levels (two tailed p-values)
1	Apr 01,1998 – Oct 11, 1998	0.099
2	Oct 21, 1998 – May 01, 1999	0.026
3	May 11, 1999 – Nov 21, 1999	0.473
4	Dec 01, 1999 – Jun 11, 2000	0.223
5	Jun 21, 2000 – Jan 01, 2001	0.055
6	Jan 11, 2001 – Jul 21, 2001	0.229
7	Aug 01, 2001 – Feb 11, 2002	0.285
8	Feb 21, 2002 – Sep 01, 2002	0.425
9	Sep 11, 2002 – Mar 21, 2003	0.473
10	Apr 01, 2003 – Oct 11, 2003	0.33
11	Oct 21, 2003 – May 01, 2004	0.457
12	May 11, 2004 – Nov 21, 2004	0.163
13	Dec 01, 2004 – Jun 11, 2005	0.317
14	Jun 21, 2005 – Jan 01, 2006	0.465
15	Jan 11, 2006 – Jul 21, 2006	0.379
16	Aug 01, 2006 – Feb 11, 2007	0.116
17	Feb 21, 2007 – Sep 01, 2007	0.365
18	Sep 11, 2007 – Mar 21, 2008	0.081

4.1.2. Within class change evaluation

Unsupervised classification

The result of applying divergence statistics to 85 signatures files and find the optimal value for selecting the number of classes ran by the unsupervised classification is shown in
Figure 7.

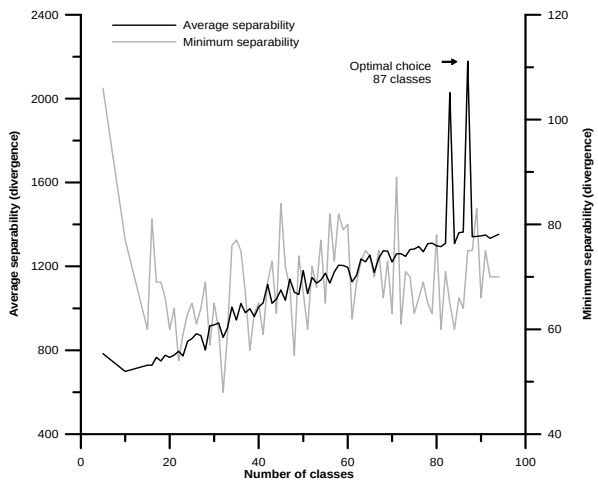

Figure 7. Selection of the optimal number of classes used to perform the unsupervised classification.

Two peaks over the average separability profile are depicted in figure above. The last of those correspond to the signature file with 87 classes. The value for the minimum separability showed that this peak is coincident with a higher value in this profile. The latter condition did not show in the first peak, where actually it is coincident with a minimum value. Thus, the signature file of the unsupervised classification of 87 classes was then selected for further analysis.

Visual assessment

No visually patterns were found for within classes. Yearly values appear to occur with no clear trends or possible grouping of years. It was observed that a high variability of the year values within a class during the winter period exist; only class 6 did not show this tendency (see Figure 8a).

The first 20 values of each year were used to statistically test for similarities among the yearly averaged value of each class. The excluded 16 points from each year represent the higher variability of autumn and winter. Only 32 out of 87 classes were found to have at least one year that was significantly different to the yearly averaged values of the class. The results and statistics of the Mann-Whitney U-test are found in appendices 8.2 and 8.3.

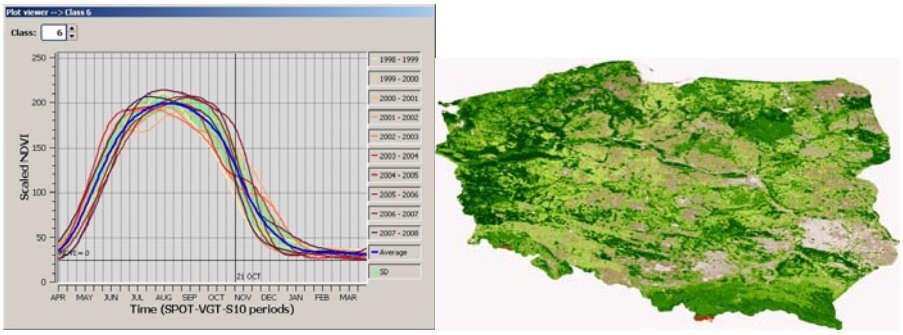

(a)

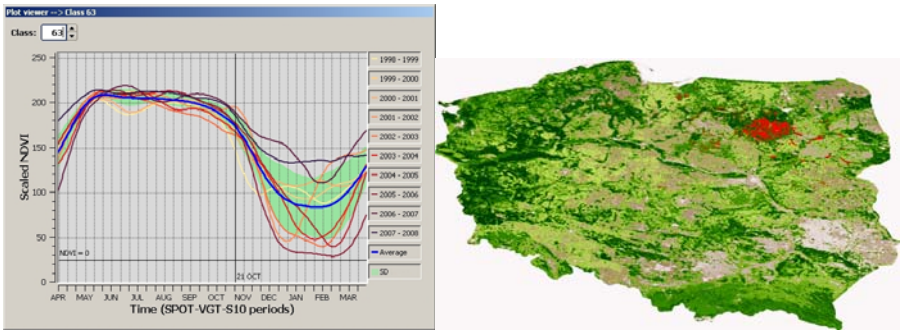

(b)

Figure 8. Selected examples of yearly variability within a class.
Maps on the left showed in red the spatial location of the related class. These images are the result of the unsupervised classification with 87 classes. In (a), all years were proved to be similar. In the other hand, (b) represents a class where anomalous years were proved to occur.

4.1.3. Class similarities evaluation through a Key Index

The combination of all unique pair of classes were used to cross tabulate the Key Index for each paired classes compared. The frequencies of the Key Index were plotted using a histogram with 10 bins (see Figure 9). The range defined by the two last two bins were used to set the threshold for similarity.

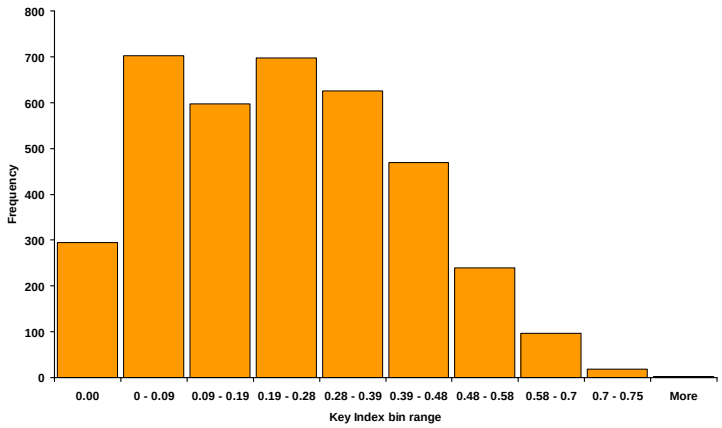

Figure 9. Histogram showing the frequency of the calculated Key Index used to set the threshold of Key Index similarity.

A threshold value with Key Index >= 0.7 was obtained. Using this condition in the upper-diagonal crossing table out of 87 classes, 8 merged classes were defined from 20 similar classes. Thus, 75 classes remained in the signature file. The Table 5 shows the classes merged and their corresponding group, whereas in Table 6 a selected part of the cross tabulated matrix had been shown.

Table 5. Groups and classes selected by using the Key Index for similarity.

Group	Classes merged
1	5, 10
2	9, 11
3	13, 22
4	17, 21
5	30,34,35,37,42,52
6	28, 36
7	39, 61
8	53, 57

Table 6. Table showing part of the matrix used to merge classes that surpassed the Key Index threshold of 0.7. Two different colours of orange are used to show different groups to merge. Columns and rows of selected classes are shown in yellow to facilitate the group visualization.

Classes	34	35	36	37	38	39	40	41	42	...	52
25	0.45	0.54	0.32	0.62	0.19	0.39	0.10	0.45	0.57	...	0.54
26	0.36	0.21	0.44	0.24	0.40	0.21	0.59	0.31	0.25	...	0.30
27	0.42	0.32	0.49	0.36	0.49	0.32	0.32	0.46	0.37	...	0.45
28	0.61	0.36	**0.85**	0.43	0.58	0.27	0.31	0.47	0.39	...	0.47
29	0.40	0.23	0.49	0.26	0.52	0.24	0.51	0.34	0.28	...	0.34
30	**0.73**	0.57	0.52	0.67	0.36	0.35	0.19	0.58	0.56	...	**0.75**
31	0.62	0.47	0.55	0.51	0.37	0.32	0.20	0.66	0.44	...	0.46
32	0.47	0.60	0.30	0.60	0.22	0.55	0.15	0.44	0.59	...	0.57
33	0.47	0.26	0.54	0.31	0.55	0.27	0.43	0.43	0.33	...	0.38
34	1	0.47	0.54	0.56	0.40	0.29	0.22	0.64	0.48	...	0.59
35		1	0.36	**0.74**	0.21	0.47	0.11	0.48	0.66	...	0.58
36			1	0.42	0.58	0.26	0.33	0.41	0.37	...	0.45
37				1	0.25	0.42	0.12	0.55	**0.73**	...	**0.72**
38					1	0.16	0.42	0.33	0.26	...	0.34
39						1	0.1	0.34	0.47	...	0.35

In Figure 10 is shown an overlay of classes 28 and 36 that after being considered similar using the Key Index had been merged into a single spectrum.

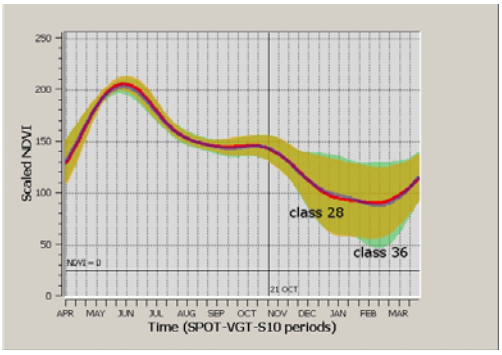

Figure 10. Visualisation of merged group 6: classes 28 (in brown-orange) and 36 (in green). The red line represents the mean values of class 28, and the blue line mean profile of class 36. It is evident that both classes can be considered as similar.

4.1.4. Library extraction

Supervised classification

The supervised classified image of Poland using the reference library of 75 classes (MLC_75C) is shown in Figure 11.

Library expression

The cross-tabulated table with the 75 classes of the reference library and CORINE Land Cover 2000 (CLC2000) can be reviewed in appendix 8.4. This table is the source of the unique legend of the 75 unique classes. Figure 11shows the resulting map.

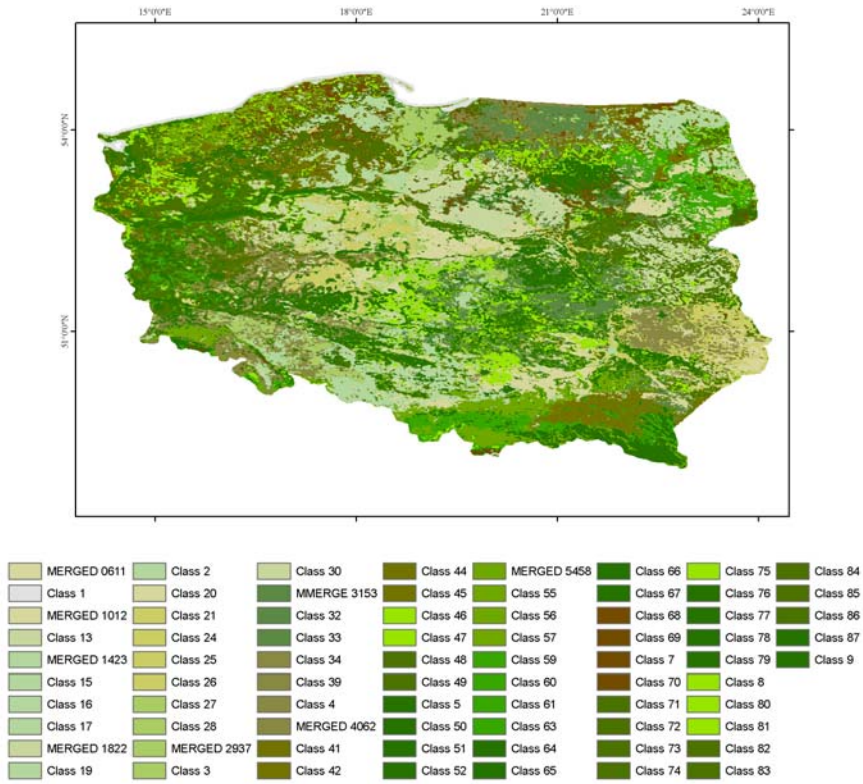

Figure 11. Map of Poland showing the 75 classes of the reference library over a 10 year period. The correspondence of this legend with CORINE Land Cover 2000 level 2 classes, can be found in appendix 8.4 and 8.5.

5. Discussions

In the introduction section was mention that the NDVI tends to be negative biased when compared the reflectance values measured by the satellite at the TOA to those values measured on the ground-TOC. Hird and McDermid (2009) advice the users of NDVI time series datasets to: *"…consider carefully their ultimate objectives and the nature of the noise present in an NDVI data set when selecting an approach to noise reduction"*.

The later authors through an empirical analysis determined which of six selected NDVI noise reduction techniques performed best under given conditions, and revealed the general superiority of two function-fitting methods: the double logistic of Beck et al., (2006) and the asymmetric Gaussian technique of Jönsson and Eklundh (2002). The general aim in both studies was to derive parameters related to vegetation phenology and production.

This study showed that, forcing an upper envelope to all but the last of four iterations while the adaptive moving window of the Savitzky-Golay filter is suppressing disturbances to reduce NDVI noise, the resulting profile maintain the seasonal variations of NDVI whiteout smoothing to much the original data.

This result is considered to be sufficient to fulfil the objective 1 of this research. The logic of the methodology is kept as long as the resulting profile maintains the seasonal variations of the response of the vegetation with reasonable values at TOA as can been seen in Figure 6. Thus, it could be applied regardless the method used to reduce the NDVI noise.

The principle of parsimony was the main reason to choose this filter among those suggested by Hird and McDermid (2009). The simplicity of the ASAVGOL filter, allowed in this study a fast modification of its code to force the adaptation of the upper envelope to the NDVI data and account for the negatively biased noise.

The effect of the extreme variability in weather conditions in Poland during autumn and winter, can mislead the evaluation of within class change. Furthermore, along with weather anomalies, this variability may also include changes due to vegetation phenology (de Bie, 2002, Cleland et al., 2007). Figure 4 shows that this variability occurs after the period of Oct 21, increasing during winter.

The yearly arrangement of the time-series allowed a better visual interpretation of the results. Even though there was no visible pattern in the graduated colours of each year; it was possible to observe that the curves followed the same behaviour. However, depending on the trained eye of the observer, some anomalies may be detected providing bias to the analysis.
To avoid this bias (due to human perception), the Mann-Whitney U-test was used to test for similarities among the yearly averaged value of each class. By excluding the 16 points from each year that represent this higher variability, 20 values of each year were used to run the test (see results in appendix 8.2). The result of this method is the first indication of classes, where tendency of change can be detected. This proved to be useful in detecting individual years within a class; that were significantly different from the yearly averaged values of the class.

This research formulated a Key Index that, allowed a user to test whether two pairs of averaged years (within a class) were similar. The standard deviation (of the NDVI values in a time-series) has been used to address inter-annual variation of years that are actually stable or highly variable (Oindo et al., 2000). However, there is currently no available literature that outlines a weighting system that can be used to weight the intersection of the line distances, as defined between the lower and upper limits of the standard deviation of paired classes (the principle of the Key Index). Generally, in medium or high latitudes that are prone to snow, it is difficult to detect change (Beck et al, 2006). The use of the Key Index proved to be useful, in detecting classes that are similar in behaviour, regardless of the inter-annual variability of the classes.

This research showed two methods that proved to be useful for library extraction of hyper-temporal NDVI images. The library building by class merging, follows the logic used by de Bie et al. (2008) and Ramoelo (2007). However, in this research, the logic was generalized and developed further (e.g. by not limited to 1 or 2 years period, like in Ramoelo, 2007). The proposed methodology of this research showed how a user can extract unique annual profiles, and express the signature library in a data file as required when mapping changes with multiple applications (such as land cover change, monitoring vegetation dynamics or crop monitoring).

The library building by temporal spectrum merging method, was unable to perform a supervised maximum likelihood classification (using the reference library), due to the current limitations of available software. The software options available to perform classification by means of a spectral library, requires that a confusion matrix is attached (e.g. Maximum Likelihood Classification). This raises the problem of coping with mixed pixels. The latter was out of the scope of this research. This research showed that is possible to build a legend, using a unique reference library, derived from the data itself. This legend is subsequently related with actual objects or features in reality, and may be used to create RS-based change maps.

5.1. Limitations

One key limitation identified was the necessity for further research regarding cloudy areas and neighbouring pixels. There is also a need to address the issue of light anisotropic effects.

6. Conclusions

- The research showed that by using a modified version of the adaptive Savitzky-Golay filter to force an upper envelope to a NDVI time-series, it is possible to obtain a streaming film of sequential images which are smooth and without shocks, and is representative for the 'good' original values.
- The research showed that, with a confidence level of 95%, in a NDVI noise-reduced time series it is possible to detect individual years within a class that are significantly different from the yearly averaged values of the class. This follows the removal of periods of high variability caused by snow.

- The research showed that by using a Key Index (based on the averaged years within a class), it is possible to derive a threshold to measure the similarity of the curves. This involved using the weighted lengths of the intersection of the line distances, defined between the lower and upper limits of the standard deviation of paired classes. Pairs of classes surpassing the Key Index threshold can be merged regardless of the inter-annual variability, provided they show that they were similar in behaviour.

- This research showed that unique annual profiles could be extracted by class merging signature files, regardless of inter-annual variability. This could be achieved only when those signatures had shown that they were similar in behaviour.

7. References

Bakker, W.H. and Schmidt, K.S., 2002. Hyperspectral edge filtering for measuring homogeneity of surface cover types. ISPRS Journal of Photogrammetry and Remote Sensing, 56(4).

Bates, B.C., Kundzewicz, Z.W., Wu, S., Palutikof, J.P. and Eds., 2008. Climate Change and Water, Technical Paper of the Intergovernmental Panel on Climate Change. IPCC Secretariat, Geneva, pp. 210.

Beck, P.S.A., Atzberger, C., Høgda, K.A., Johansen, B. and Skidmore, A.K., 2006. Improved monitoring of vegetation dynamics at very high latitudes: A new method using MODIS NDVI. Remote Sensing of Environment, 100(3): 321-334.

Beck, P.S.A., Wang, T.J., Skidmore, A.K. and Liu, X.H., 2008. Displaying remotely sensed vegetation dynamics along natural gradients for ecological studies. International Journal of Remote Sensing, 29(14): 4277 - 4283.

Bontemps, S., Bogaert, P., Titeux, N. and Defourny, P., 2008. An object-based change detection method accounting for temporal dependences in time series with medium to coarse spatial resolution. Remote Sensing of Environment, 112(6): 3181-3191.

Bradley, B.A., Jacob, R.W., Hermance, J.F. and Mustard, J.F., 2007. A curve fitting procedure to derive inter-annual phenologies from time series of noisy satellite NDVI data. Remote Sensing of Environment, 106(2): 137-145.

Chen, J. et al., 2004. A simple method for reconstructing a high-quality NDVI time-series data set based on the Savitzky-Golay filter. Remote Sensing of Environment, 91(3-4): 332-344.

Cleland, E.E., Chuine, I., Menzel, A., Mooney, H.A. and Schwartz, M.D., 2007. Shifting plant phenology in response to global change. Trends in Ecology & Evolution, 22(7): 357-365.

de Bie, C.A.J.M., 2002. Novel approaches to use RS - products for mapping and studying agricultural land use systems. In: ISPRS 2002 TC - VII : Commission VII, Working Group VII-2.1 on sustainable agriculture : International symposium on resource and environmental monitoring : 3-6 December 2002, Hyderabad. 9 p.

de Bie, C.A.J.M., Bouma, J.P. and Driessen, P.M.P., 2000. Comparative performance analysis of agro - ecosystems, ITC, Enschede, 232 pp.

de Bie, C.A.J.M., Khan, M.R., Toxopeus, A.G., Venus, V. and Skidmore, A.K., 2008. Hypertemporal image analysis for crop mapping and change detection. In: ISPRS 2008 : Proceedings of the XXI congress : Silk road for information from imagery : the International Society for Photogrammetry and Remote Sensing, 3-11 July, Beijing, China. Comm. VII, WG VII/5. Beijing : ISPRS, 2008. pp. 803-812.

de Bie, C.A.J.M. and Nidumolu, U.B., 2004. Mapping land use through multi - temporal NDVI image data and knowledge on practiced local crop calendars : abstract. In: Proceedings of the 2nd international SPOT VEGETATION users conference, March 24-26 2004, Antwerp. pp. 88.

Duggin, M.J. and Robinove, C.J., 1990. Assumptions Implicit in Remote-Sensing Data Acquisition and Analisis. International Journal of Remote Sensing, 11(10): 1669-1694.

Fung, T. and Siu, W., 2000. Environmental quality and its changes, an analysis using NDVI. International Journal of Remote Sensing, 21(5): 1011-1024.

Guo, Z., Li, Y. and Gan, Y., 2003. Spatial Pattern of Ecosystem Function and Ecosystem Conservation. Environmental Management, 32(6): 682-692.

Hermance, J.F., 2007. Stabilizing high-order, non-classical harmonic analysis of NDVI data for average annual models by damping model roughness. International Journal of Remote Sensing, 28(12): 2801 - 2819.

Hermance, J.F., Jacob, R.W., Bradley, B.A. and Mustard, J.F., 2007. Extracting Phenological Signals From Multiyear AVHRR NDVI Time Series: Framework for Applying High-Order Annual Splines With Roughness Damping. Geoscience and Remote Sensing, IEEE Transactions on, 45(10): 3264-3276.

Hird, J.N. and McDermid, G.J., 2009. Noise reduction of NDVI time series: An empirical comparison of selected techniques. Remote Sensing of Environment, 113(1): 248-258.

Jain, A.K. and Dubes, R.C., 1988. Algorithms for clustering data. (Prentice Hall advanced reference series). Prentice-Hall, Englewood Cliffs etc., 320 pp.

Jones, K.B. et al., 1997. An Ecological Assessment of the United States Mid-Atlantic Region: A Landscape Atlas. United States Environmental Protection Agency. Office of Research and Development, Washington DC, 20460. EPA/600/R-97/130.

Jönsson, P. and Eklundh, L., 2002. Seasonality extraction by function fitting to time-series of satellite sensor data. Geoscience and Remote Sensing, IEEE Transactions on, 40(8): 1824-1832.

Jönsson, P. and Eklundh, L., 2004. TIMESAT--a program for analyzing time-series of satellite sensor data. Computers & Geosciences, 30(8): 833-845.

Kerr, J.T. and Ostrovsky, M., 2003. From space to species: ecological applications for remote sensing. Trends in Ecology & Evolution, 18(6): 299-305.

Kruskal, W.H. and Wallis, W.A., 1952. Use of Ranks in One-Criterion Variance Analysis. Journal of the American Statistical Association, 47(260): 583-621.

Lambin, E.F. and Linderman, M., 2006. Time series of remote sensing data for land change science. Geoscience and Remote Sensing, IEEE Transactions on, 44(7): 1926-1928.

Lu, D., Mausel, P., BrondÃ-zio, E. and Moran, E., 2004. Change detection techniques. International Journal of Remote Sensing, 25(12): 2365-2401.

MacFarland, T.W., 1998. Mann-Whitney U-Test-Tutorial. Available from: http://www.nyx.net/~tmacfarl/STAT_TUT/mann_whi.ssi [Accessed: October 2008].

Memarsadeghi, N., Mount, D.M., Netanyahu, N.S. and Le Moigne, J., 2003. A fast implementation of the ISOCLUS algorithm, Geoscience and Remote Sensing Symposium, 2003. IGARSS '03. Proceedings. 2003 IEEE International, pp. 2057-2059.

Milton, R.C., 1964. An Extended Table of Critical Values for the Mann-Whitney (Wilcoxon) Two-Sample Statistic. Journal of the American Statistical Association, 59(307): 925-934.

Nemani, R. and Running, S., 1997. Land cover characterization using multitemporal red, near-IR, and thermal-IR data from NOAA/AVHRR. Ecological Applications, 7(1): 79-90.

Nogues-Bravo, D., Araujo, M.B., Romdal, T. and Rahbek, C., 2008. Scale effects and human impact on the elevational species richness gradients. Nature, 453(7192): 216-219.

Pettorelli, N. et al., 2005. Using the satellite-derived NDVI to assess ecological responses to environmental change. Trends in Ecology & Evolution, 20(9): 503-510.

Savitzky, A. and Golay, M.J.E., 1964. Smoothing and Differentiation of Data by Simplified Least Squares Procedures. Anal. Chem., 36(8): 1627-1639.

Schmidt, K.S. and Skidmore, A.K., 2003. Spectral discrimination of vegetation types in a coastal wetland. Remote Sensing of Environment, 85(1): 92-108.

Skidmore, A.K. et al., 2006. Herpetological species mapping for the Mediterranean. In: ISPRS 2006 : ISPRS mid-term symposium 2006 remote sensing : from pixels to processes, 8-11 May 2006, Enschede, the Netherlands. Enschede : ITC, 2006. 7 p.

Tou, J.T. and Gonzalez, R.C., 1974. Pattern recognition principles. (Applied mathematics and computation ; 7). Addison-Wesley, Reading etc., 377 pp.

UNEP, 2007. Global Environmental Outlook - 4 GEO, United Nations Environment Programme, Nairobi.

Zhou, Q., Li, B. and Kurban, A., 2008. Trajectory analysis of land cover change in arid environment of China. International Journal of Remote Sensing, 29(4): 1093-1108.

Online Sources:

Central Statistical Office, 2008. Area and Population in the Territorial Profile in 2008. Available from: http://www.stat.gov.pl/gus/index_ENG_HTML.htm [Accessed: February 2009].

Poland Gateway, 2006. Climate. Available from: http://travel.poland.com/ [Accessed: February 2009].

VEGETATION Program. Available from http://www.spot-vegetation.com/ [Accessed: February 2009].

8. Appendices

8.1. Python code of the modification of the Adaptive Savitzky-Golay filter, based on the fortran and matlab code of the work done by Jönsson and Eklundh, (2004).

```
 #! /usr/bin/env python
'''
pyTIMESAT --> TIMESAT implentation for python 2.5
AUTHOR: Jose M. Beltran(gemtoolbox@gmail.com)
PURPOSE: Applies a modification of the adaptive Savitzky-Golay filter
      following the TIMESAT v2.3 implementation with optional upper envelope
      forcing. To be used with SPOT VEG NDVI 10-day synthesis.
NOTE:    TIMESAT v2.3. A package for processing time-series of satellite sensor
      data.
       Authors:
       Per Jonsson, Malmo University, Sweden,
         e-mail per.jonsson@ts.mah.se
       Lars Eklundh, Lund University, Sweden,
         e-mail lars.eklundh@nateko.lu.se )

REQUIRES: numpy, GDAL, Gnuplot, scipy, and GEMtoolBox
WARNING: Only complete yearly stack of images should be used as an input.
      e.g. 10 years, 9 years; but no 9 years with 8 months.


Updated: Nov 03,2008
'''
import osgeo.gdal as og, osgeo.gdal_array as oga
import numpy as np
import osgeo.gdalconst as ogc
from scipy import r_ as r_
from scipy import c_ as c_
import time
import GEMtoolBox as gem
import Gnuplot

t0=time.clock()
# ---
def spike(y,w,spikecutoff = 0.5):
   '''
   A spikecutoff will be used as: spikecutoff * y[y>0].std(). A value of 2 is
   the normal value  for TIMESAT. But in TIMESAT they used
```

```
    spikecutoff * y.std(). I suggest to use only the values of y>0 to
    calculate the distance. A value lower than 1 will pick up more spikes.
    '''
    w0 = np.ravel(w.copy())
    # Preserving the old weight values. This could be done directly over w.
    spikes = np.zeros(nb)
    ymean = y[y>0].mean()
    ystd = y[y>0].std()
    wmax = w0.max()
    dist = spikecutoff*ystd
    swinmax = int(np.floor(nptperyear/7))
    leftSlice = slice(nb-swinmax,nb)
    rightSlice = slice(0,swinmax)

    wext = np.ravel(r_[w0[leftSlice],w0,w0[rightSlice]])
    yext = np.ravel(r_[y[leftSlice],y,y[rightSlice]])
    # find single spikes and set weights to zero
    for i in range(swinmax,nb+swinmax):
        m1 = i - swinmax
        m2 = i + swinmax + 1

        idx_wext_nonzero = wext[slice(m1,m2)].nonzero()
        index = m1 + idx_wext_nonzero[0]
        med = np.median(yext[index])
        if abs(y[m1] - med) >= dist and ((y[m1] < (float(yext[i-1])+\
        float(yext[i+1]))/2 - dist) or (y[m1] > max(yext[i-1],yext[i+1])+dist)):
            w0[m1] = 0
            spikes [m1] = 1
            pass
        pass
    return w0,spikes
# ---

# ---
def savgol(y,w):
    ''' Adapted code from TIMESAT '''
    # Preventing modifications on the source profile
    y_ = y.copy()
    w_ = w.copy()
    winmax = win.max()
    # Extend data circularity to improve fitting near the boundary
    # of original data
    t = np.arange(-winmax+1,nb + winmax+1)
    leftSlice = slice(nb-winmax,nb)
    rightSlice = slice(0,winmax)
    # ---
    y_ = r_[y_[leftSlice], y_,y_[rightSlice]]#[:,:,np.newaxis]
    # Need it to convert to 1D to be dimensions-compatible with the yfits
```

```
yfit = np.ravel(y_)
wfit = r_[w_[leftSlice],w_,w_[rightSlice]]
# general slice which points always to the profile data
dataSlice = slice(winmax, nb + winmax)
dataRange = range(winmax, nb + winmax)
# number of elements in tuple of indices resulting
# during the following fitWindowAt
idx_t = 2
nenvi = len(win) # number of fitting windows-nenvi)
#
yfits = np.zeros((nb,nenvi))
#
for ienvi in range(nenvi):
   # Compute standard deviation for fitted function
   yfitstd= np.std(yfit[:])
   for i in dataRange:
      # set fitting window
      m1 = i-win[ienvi]
      m2 = i+win[ienvi]+1
      left = 0
      right = 0
      # Adapting fitting interval. Large variation use a smaller window.
      adjustWindow = ((yfit[slice(m1,m2)].max() -\
            yfit[slice(m1,m2)].min()) > 1.2 * 2 * yfitstd)
      if adjustWindow == True:
         # adjusting the left side with views of m1
         m1 = m1 + int(np.floor(win[ienvi])/3)
         # adjusting the right side with views of m2
         m2 = m2 - int(np.floor(win[ienvi])/3)
         pass
      # Check so that there are enough points, at least 3 at either side
      # with weights different from zero. If not, extend fitting window
      failleft = 0
      while  (abs(wfit[slice(m1,i+1)]) > 1e-10).sum() \
                                    < 3 and failleft ==0:
         m1 = m1 -1
         if m1 < 1:
            failleft = 1
            m1 = 1
            left = left +1
            #print 'extended on left '+str(left)
            pass
         pass
      failright = 0

      while (abs(wfit[slice(i,m2)]) > 1e-10).sum() < 3 and failright == 0:
         m2 = m2+1
         if m2 > nb + 2*winmax:
```

```
                failright = 1
                m2 = nb + 2*winmax
                right = right+1
                #print 'extended on right '+str(right)
                pass
            pass
        # Fit the polynomial if enough data values with non-zero weight
        if failleft ==0 and failright == 0:
            # preparing data slices as to construct the design matrix
            s_wfit = np.ravel(wfit[slice(m1,m2)])
            s_t = t[slice(0,m2-m1)]
            s_y = np.ravel(y_[slice(m1,m2)])
            # Construct the design matrix A and the column matrix b
            A = c_[np.matrix(s_wfit).T,np.matrix(s_wfit*s_t).T,\
                np.matrix(s_wfit*s_t**2).T]
            b = np.matrix(s_wfit*s_y).T
            # Solving linear-squares problem A^TAc = A^Tb
            ATA = (A.T)*A
            ATb = (A.T)*b
            #
            c = np.linalg.solve(ATA, ATb)
            # Evaluating the fitted function
            yfit[i] = c[0] + c[1]*t[i-m1] + c[2]*t[i-m1]**2
        else:
            s_y = np.ravel(y_[slice(m1,m2)])
            yfit[i] = np.median(s_y)
            pass
        ####################################
        ## CORE modification                    ####
        if forceUpperEnvelope == True:
            # All iterations will be forced to the upper envelope
            if lastIterationLikeTIMESATfit == False:
                if (yfit[i] < y[i-winmax])and wfit[i]==1:
                    yfit[i] = y[i-winmax]
            # All except the last iteration
            # will be forced to the upper envelope
            else:
                if (yfit[i] < y[i-winmax])and wfit[i]==1 and \
                    ienvi<win.shape[0]-1: yfit[i] = y[i-winmax]
                pass
            pass                                    ####
        ####################################
        yfits[:,ienvi] = yfit[dataSlice]
        pass
    pass
  return yfits
# ---
def plot(pRow,pCol):
```

```
    ''' Plot the pixel profile at (pRow,pCol), the pixel-fitted
    profile and outliers'''
    gp.clear()
    currentPixel = gem.getPixelProfile(in_dataset, idx_row = pRow ,\
                                idx_col = pCol)
    original = Gnuplot.Data(currentPixel)
    gp.title('Iterations window size: '+str(win)+' '+xtraNotes)
    gp.xlabel('Time (10-day intervals{[1st,11th,21th] of each month}')
    gp.ylabel('Scaled NDVI')
    original.set_option(with_='lines lc rgb "purple" lw 1')
    original.set_option(title = 'original data')
    # ---
    lastIteration = Gnuplot.Data(holder[:,pRow,pCol])
    lastIteration.set_option(with_='lines lc rgb "red" lw 2')
    lastIteration.set_option(title = 'Last iteration in window')
    olier = Gnuplot.Data(outliers[:,pRow,pCol])
    olier.set_option(title = 'Outliers')
    #
    gp.plot(original,lastIteration,olier)
    # ---
    pass

# ---

t1=time.clock()
# Opening working image
#workingPath = 'D://working//results//'
#src_filename = 'im3r4c_324b.img' # dice360b_1_1.img # sp_1_1.img
print 'WARNING:'
print 'Only complete yearly stack of images should be used as an input.'
print 'e.g. 10 years, 9 years, etc...'
print 'do not use stacks like 9 years with 8 months,'
print 'this will affect the circularity of the data'
print ''

workingPath = raw_input('PATH of the source image- WORKING PATH \
                            ( D://working//path// ) :')
src_filename = raw_input('SOURCE IMAGE filename ( filename.img ): ')

print 'Opening source image ...'
in_dataset = og.Open(workingPath+src_filename)
# nr -- number of rows, nc -- number of columns, nb = number of bands
nr,nc,nb = gem.getImageDim(in_dataset)
print 'Dimensions: '+ str(nr)+' rows, '+str(nc)+' cols, '+ str(nb)+' bands'
# out_dataset requires to be set as a global \
#to avoid opening it multiple times in the loop for saving
out_filename = raw_input('Working with image: '+src_filename+\
                ', Give OUTPUT IMAGE filename:')
```

```
print 'Creating the image holder for image: '+out_filename+' in: '+workingPath
outfilenamePlusPath = workingPath+out_filename
# ------
spikecutoff = 0.5
# Setting the window values for the adaptive Savitzky-Golay filter
win = np.array([1,2,3,4])
try:
   windows = input('Give the Savitzky-Golay window sizes \
      for each of the fitting steps, default values: [1,2,3,4]')
   win = np.array(windows)
except:
   print 'Using default values: [1,2,3,4]'
   pass


forceUpperEnvelope = True  # Kees de Bie Suggestion
try:
   forceUp = input('Force upper envelope [True or False],\
                  default value is [True] "case sensitive": ')
   forceUpperEnvelope = forceUp
except:
   print 'Using default value: True'
   pass

lastIterationLikeTIMESATfit = True # Kees de Bie Suggestion
try:
   lastlike = input('Apply regular TIMESAT fit for the last iteration\
                   [True or False], default is [True] "case sensitive": ')
   lastIterationLikeTIMESATfit = lastlike
except:
   print 'Using default value: True'
   pass


print ''
print 'Initiating  variables ...'
# Initiate matrices that will contain time series
# for all pixels (columns in a row)
rmatrix = np.zeros((nb,nc)) # Row matrix
# Initiate vectors that will hold the time series for a pixel
y = np.zeros(nb)
displayEstimatedTime = True
outliers=np.empty((nb,nr,nc))
# ---
nptperyear = 36
# variable to hold all the filtered values of y for each iteration
y1 = np.zeros((nb,win.shape[0]))
rowHolder = np.zeros((nb,nc))
```

```
# Holder will store all the fitted values in a 3d array.
holder = np.zeros((nb,nr,nc))
# ---
t2=time.clock()
print t2-t1, 'seconds so far.'
print ' Here we go ... '

# ---LOOPING for all rows
for irow in range(nr):
   # Read the time-series for all pixels in row
   rmatrix = gem.getRowProfile(in_dataset, idx_row=irow)
   #----
   for icol in range(nc):
      # LOOPING AMONG ALL COLUMNS
      w = np.ones(nb)
      y = rmatrix[:,icol] # [nb,nc]
      # The accepted range of values are 2:254
      # all other values are set to zero.
      w[y<2] = 0
      # Time-series with too many data values with zero weight
      # are not processed
      missingdata = 0
      if w[w == 0].shape[0] >= np.floor(3*nb/4): missingdata = 1
      #
      for k  in range(0,nb+1-int(np.floor(nptperyear/3))):
         sk = slice(k,int(k+np.floor(nptperyear/3)))
         if abs(w[sk].sum()) == 0: missingdata = 1
         pass
      if missingdata == 0:
         t3=time.clock()
         # Identify spikes in the time-series and #
         # set the corresponding weights to zero
         ws,outlier = spike(y, w, spikecutoff)
         outliers[:,irow,icol] =outlier*y
         # Iterative Savitzky-Golay filtering
         # to adopt to upper (or lower) envelope  of the time-series.
         y1 = savgol(y,ws) # y1.shape is [nb,nenvi]
         if displayEstimatedTime == True:
            t4=time.clock()
            timediff = t4-t3
            estimatedHrs = ((timediff * nr* nc)/60)/60
            print 'Elapsed time by cleaning one pixel: ',timediff,\
                                 ' seconds'
            print 'Estimated time: ', timediff * nr *nc /60, \
                     ' minutes, or: ', estimatedHrs,' hours, to finish'
            displayEstimatedTime = False
            pass
```

```
        else:
            y1[:,:] = 0 # The profile is set to zero.
            print 'temporal profile in row: '+str(irow)+', col: '+str(icol)+\
                  ' had been set to zero.'
            pass

        holder[:,irow,icol] = y1[:,win.shape[0]-1] #
        pass

    print 'row : ', irow, ' of: ',nr

    pass

gem.array3DToImage(holder,outfilenamePlusPath,in_dataset)
# ---
# Read the time-series for all pixel in the image


t5=time.clock()
print 'Total looping time: ', (t5-t2)/60, 'minutes, ', (t5-t2)/60/60,' hours.'
# -----
# -----
if forceUpperEnvelope == True:
    if lastIterationLikeTIMESATfit == True:
        xtraNotes = ' SAVGOL-TIMESAT with all but the last, UENV-forced'
        pass
    else:
        xtraNotes = ' SAVGOL-TIMESAT with forced UENV'
        pass
    pass
else:
    xtraNotes = ' Upper Envelope (UENV) Savitzky-Golay filter (SAVGOL) \
        TIMESAT-based approach'
    pass

#
# Ready to plot
gp = gem.initGraphics()

# -------------------------------------------------------
#in_dataset = None
print 'Done.'
print 'use the plot(row,col) to plot the pixel profile'
#plot(0,0)
```

8.2. Within class change- classes with anomalous years

Within class change. If a year period was found to be similar to the mean of the class, then 1 else 0.
A grey background over the class cell represents classes where at least one year was found to be significantly different from the mean of the class.

	Period									
Class	**1998-1999**	**1999-2000**	**2000-2001**	**2001-2002**	**2002-2003**	**2003-2004**	**2004-2005**	**2005-2006**	**2006-2007**	**2007-2008**
1	1	0	1	0	1	1	0	1	1	1
2	1	1	1	1	1	1	1	1	1	1
3	0	1	1	1	1	1	1	1	1	1
4	1	1	1	1	1	1	1	1	1	1
5	1	1	1	1	1	1	1	1	1	1
6	1	1	1	1	1	1	1	1	1	1
7	1	1	1	1	1	1	1	1	1	1
8	1	1	1	1	1	1	1	1	1	1
9	1	1	1	1	1	1	1	1	1	1
10	1	1	1	1	1	1	1	1	1	1
11	1	1	1	1	1	1	1	1	1	1
12	1	1	1	1	1	1	1	1	1	1
13	1	1	1	1	1	1	1	1	1	0
14	1	1	1	1	1	1	1	1	1	1
15	1	1	1	1	1	1	1	1	1	1
16	1	1	1	1	1	1	1	1	1	1
17	1	1	1	1	1	1	1	1	1	1
18	1	1	1	1	1	1	1	1	1	1
19	1	1	1	1	1	1	1	1	1	1
20	1	1	1	1	1	1	1	1	1	1
21	1	1	1	1	1	1	1	1	1	1
22	1	1	1	1	1	1	1	1	1	1
23	1	1	1	1	1	1	1	1	1	1
24	1	1	1	1	1	1	1	1	1	1
25	0	1	1	1	1	1	1	1	1	0
26	1	1	1	1	1	1	1	1	1	1
27	1	1	1	1	1	1	1	1	1	1
28	1	1	1	1	1	1	1	1	1	1
29	1	1	1	1	1	1	1	1	1	1
30	1	1	1	1	1	1	1	1	1	1
31	1	1	1	1	1	1	1	1	1	1
32	1	1	1	1	1	1	1	1	1	1
33	1	1	1	1	1	1	1	1	1	1
34	1	1	1	1	1	1	1	1	1	1
35	1	1	1	1	1	1	1	1	1	1
36	1	1	1	1	1	1	1	1	1	1
37	1	1	1	1	1	1	1	1	1	1
38	1	1	1	1	1	1	1	1	1	1
39	1	1	1	1	1	1	1	1	1	0
40	1	1	1	1	1	1	1	1	1	1
41	1	1	1	1	1	1	1	1	1	1
42	1	1	1	1	1	1	1	1	1	1
43	1	1	1	1	1	1	1	1	1	1
44	1	1	1	1	1	1	1	1	1	1
45	1	1	1	1	1	1	1	1	1	1
46	1	1	1	1	1	1	1	1	1	0
47	1	1	1	1	1	1	1	1	1	1
48	1	1	1	1	1	1	1	1	1	1
49	1	1	1	1	1	1	1	1	1	1
50	1	1	1	1	1	1	1	1	1	1
51	1	1	1	1	1	1	1	1	1	1
52	1	1	1	1	1	1	1	0	1	1
53	1	1	1	1	1	1	1	1	1	0
54	1	1	1	1	1	1	1	1	1	1
55	1	1	1	1	1	1	1	0	0	1
56	1	1	1	1	1	1	1	1	1	1

Within class change. If a year period was found to be similar to the mean of the class, then 1 else 0.
A grey background over the class cell represents classes where at least one year was found to be significantly different from the mean of the class.

	Period									
Class	**1998-1999**	**1999-2000**	**2000-2001**	**2001-2002**	**2002-2003**	**2003-2004**	**2004-2005**	**2005-2006**	**2006-2007**	**2007-2008**
57	1	1	1	1	1	1	1	1	1	1
58	1	1	1	1	1	1	1	1	1	1
59	1	1	1	1	1	1	1	1	1	1
60	1	1	1	1	1	1	1	1	1	0
61	1	1	1	1	1	1	1	1	1	1
62	1	1	1	1	1	1	1	1	1	1
63	1	1	1	0	1	1	1	0	0	1
64	0	1	1	1	1	1	1	1	1	0
65	1	1	1	1	1	1	1	1	1	0
66	1	1	1	1	1	1	1	1	1	1
67	1	1	1	1	1	1	1	0	1	1
68	0	1	1	1	1	1	1	1	1	0
69	1	1	1	1	1	1	1	1	1	1
70	0	1	1	1	1	1	1	1	1	1
71	1	1	1	1	1	1	1	1	1	0
72	0	1	0	1	1	1	1	0	1	0
73	0	1	1	1	1	1	1	1	1	1
74	1	1	1	1	1	1	1	1	1	0
75	0	1	1	1	1	1	1	1	1	0
76	1	1	1	0	1	1	1	0	0	0
77	0	1	1	1	1	1	1	1	1	0
78	0	1	1	1	1	1	1	1	1	1
79	0	1	1	1	1	1	1	0	0	0
80	0	1	1	1	1	1	1	1	0	0
81	0	1	1	1	1	1	1	0	1	0
82	0	1	1	1	1	1	1	0	1	0
83	0	1	1	1	1	1	1	0	0	0
84	0	1	0	1	1	1	1	0	1	0
85	0	1	1	0	1	1	1	0	1	1
86	0	1	1	1	1	1	1	0	0	0
87	0	1	0	1	1	1	1	0	0	0

8.3. Within class change- two-tailed p-value for all classes

Within class change. Values represent the two-tailed p-value.
A grey background over the class cell represents classes where at least one year was found to be significantly different from the mean of the class with a significant level of 0.05**.**

	Period									
Class	**1998-1999**	**1999-2000**	**2000-2001**	**2001-2002**	**2002-2003**	**2003-2004**	**2004-2005**	**2005-2006**	**2006-2007**	**2007-2008**
1	0.144	0.025	0.402	0.045	0.978	0.117	0.028	0.552	1	0.066
2	0.079	0.194	0.499	0.745	0.705	0.204	0.534	0.16	0.766	0.204
3	0.033	0.829	0.465	0.85	0.705	0.499	0.626	0.176	0.417	0.117
4	0.552	0.808	0.725	0.372	0.871	0.387	0.892	0.665	0.892	0.234
5	0.194	0.808	0.33	0.745	0.935	0.745	0.957	0.417	0.387	0.16
6	0.482	1	0.626	0.552	0.978	0.516	0.808	0.665	0.725	0.291
7	0.626	0.685	0.433	0.387	0.516	0.725	0.705	0.607	0.291	0.344
8	0.534	0.589	0.85	0.465	0.914	0.291	0.85	0.705	0.787	0.204
9	0.552	0.745	0.705	0.589	0.871	0.516	0.935	0.745	0.552	0.194
10	0.552	0.725	0.871	0.685	0.978	0.417	0.85	0.57	0.607	0.256
11	0.85	0.787	0.725	0.85	0.387	0.344	0.358	0.433	0.607	0.13
12	0.433	0.871	0.745	0.534	0.935	0.433	0.516	0.646	0.808	0.152
13	0.372	0.534	0.304	0.417	0.766	0.387	0.705	0.665	0.372	0.045
14	0.665	0.344	0.465	0.234	0.607	0.224	0.534	0.552	0.787	0.083
15	0.607	0.829	0.808	0.871	0.344	0.482	0.33	0.465	0.552	0.144

Within class change. Values represent the two-tailed p-value.
A grey background over the class cell represents classes where at least one year was found to be significantly different from the mean of the class with a significant level of 0.05**.**

Period

16	0.291	0.552	0.552	0.935	0.957	0.685	0.935	0.33	0.245	0.279
17	0.402	0.57	0.665	1	0.626	0.978	0.402	0.646	0.978	0.105
18	0.665	0.935	0.935	0.787	0.433	0.317	0.745	0.552	0.725	0.088
19	0.449	0.808	0.957	0.646	0.892	0.185	0.871	0.402	0.499	0.304
20	0.482	0.449	0.626	0.402	0.871	0.33	0.85	0.914	0.552	0.058
21	0.465	0.224	0.665	0.402	0.957	0.137	0.935	0.85	0.787	0.11
22	0.646	0.387	0.892	0.957	0.57	0.402	0.725	0.766	0.465	0.07
23	0.665	0.234	0.705	0.957	0.344	0.317	0.482	0.57	0.725	0.152
24	0.185	0.978	0.685	0.871	0.978	0.646	0.871	0.534	0.607	0.224
25	0.016	0.465	0.123	0.808	0.871	0.499	0.978	0.152	0.256	0.005
26	0.358	0.787	0.552	0.57	0.871	0.552	0.978	0.626	0.417	0.152
27	0.358	0.787	0.914	0.499	0.646	0.137	0.829	0.256	0.417	0.279
28	0.57	0.829	0.829	0.552	0.279	0.871	0.465	0.914	0.787	0.194
29	0.304	0.317	0.57	0.589	0.957	0.256	0.871	0.482	0.433	0.051
30	0.552	0.279	0.978	0.85	0.808	0.117	0.871	0.516	0.892	0.13
31	0.402	0.871	0.787	0.935	0.482	0.402	0.829	0.534	0.607	0.066
32	0.534	0.646	0.892	0.344	0.766	0.358	0.85	1	0.57	0.079
33	0.482	0.935	1	0.892	0.291	0.626	0.317	0.589	0.516	0.099
34	0.402	0.499	0.914	0.705	0.808	0.16	0.914	0.256	0.267	0.185
35	0.304	0.482	0.935	0.433	0.892	0.33	0.935	0.482	0.33	0.117
36	0.607	0.978	0.534	0.978	0.372	0.372	0.372	0.33	0.516	0.083
37	0.57	0.465	0.534	0.224	0.607	0.256	0.626	0.725	0.482	0.051
38	0.245	0.787	0.534	0.685	0.935	0.499	0.516	0.372	0.465	0.387
39	0.291	0.279	0.685	0.465	0.978	0.144	0.685	0.267	0.705	0.037
40	0.123	0.372	0.552	0.892	0.935	0.626	0.957	0.168	0.074	0.144
41	0.267	0.433	0.935	0.957	0.725	0.176	0.871	0.256	0.705	0.204
42	0.372	0.482	0.705	0.871	0.685	0.516	0.646	0.465	0.626	0.094
43	0.387	0.589	0.705	0.85	0.957	0.499	0.808	0.372	0.344	0.279
44	0.16	0.978	0.534	0.892	0.417	0.665	0.449	0.387	0.57	0.144
45	0.267	0.725	0.465	1	0.978	0.449	0.534	0.304	0.372	0.245
46	0.417	0.626	0.914	0.358	0.646	0.358	0.725	0.914	0.387	0.023
47	0.245	0.358	0.978	0.829	0.57	0.256	0.957	0.279	0.358	0.079
48	0.245	0.705	0.57	1	0.646	0.978	0.482	0.516	0.745	0.11
49	0.16	0.787	0.449	0.914	0.745	0.646	0.829	0.433	0.402	0.094
50	0.204	0.725	0.417	0.534	0.85	0.685	0.957	0.57	0.387	0.079
51	0.234	0.417	0.871	0.516	0.829	0.372	0.871	0.499	0.234	0.055
52	0.204	0.317	0.516	0.185	0.516	0.465	0.499	0.042	0.07	0.213
53	0.402	0.626	0.589	0.685	0.829	0.57	0.607	0.914	0.534	0.04
54	0.185	0.499	0.372	0.787	0.978	0.552	0.552	0.194	0.224	0.16
55	0.168	0.387	0.204	0.213	0.935	0.534	0.185	0.033	0.037	0.213
56	0.079	0.725	0.291	0.892	0.829	0.787	0.957	0.291	0.317	0.074
57	0.33	0.808	0.829	0.685	0.665	0.665	0.552	0.417	0.626	0.137
58	0.224	0.449	0.745	0.745	0.829	0.433	0.914	0.279	0.079	0.144
59	0.079	0.808	0.117	0.626	0.402	0.766	0.234	0.088	0.417	0.051
60	0.099	0.449	0.372	0.808	0.957	0.57	0.787	0.256	0.267	0.017
61	0.123	0.516	0.317	0.358	0.85	0.646	0.402	0.055	0.07	0.083
62	0.088	0.957	0.705	0.871	0.358	0.808	0.402	0.433	0.387	0.099
63	0.291	0.344	0.291	0.028	0.372	0.85	0.267	0.02	0.03	0.099
64	0.015	0.787	0.055	0.685	0.433	0.957	0.11	0.204	0.123	0.003
65	0.055	0.534	0.185	0.57	0.766	0.766	0.892	0.417	0.176	0.013
66	0.099	0.685	0.433	0.914	0.914	0.808	0.787	0.358	0.387	0.094
67	0.234	0.589	0.449	0.088	0.725	0.85	0.317	0.045	0.062	0.344
68	0.015	0.705	0.088	0.957	0.705	0.685	0.402	0.083	0.417	0.003
69	0.07	0.808	0.33	0.745	0.871	0.871	0.433	0.213	0.745	0.099
70	0.027	0.871	0.482	0.402	0.787	0.871	0.552	0.07	0.245	0.16
71	0.144	0.344	0.829	0.957	0.646	0.279	0.787	0.213	0.516	0.025
72	0	0.787	0.033	0.465	0.829	0.417	0.978	0.008	0.117	0
73	0.033	0.57	0.402	0.534	0.935	0.914	0.892	0.11	0.13	0.099
74	0.066	0.57	0.358	0.892	0.85	0.725	0.914	0.194	0.168	0.037
75	0.006	0.465	0.117	0.176	0.787	0.685	0.57	0.051	0.176	0.045
76	0.144	0.552	0.534	0.045	0.589	0.892	0.402	0.042	0.045	0.033

Within class change. Values represent the two-tailed p-value.
A grey background over the class cell represents classes where at least one year was found to be significantly different from the mean of the class with a significant level of 0.05**.**

	Period									
77	0.014	0.449	0.185	0.516	0.978	0.685	0.935	0.055	0.062	0.023
78	0.023	0.829	0.417	0.291	0.914	0.787	0.646	0.051	0.185	0.11
79	0.003	0.256	0.083	0.123	0.725	0.176	0.745	0.025	0.015	0.005
80	0.009	0.358	0.267	0.058	0.787	0.304	0.499	0.051	0.033	0.012
81	0.006	0.665	0.256	0.433	0.871	0.534	0.358	0.035	0.344	0.045
82	0.002	0.935	0.224	0.499	0.978	0.646	0.766	0.033	0.062	0.028
83	0.001	0.685	0.094	0.978	0.685	0.935	0.552	0.028	0.033	0.001
84	0	0.402	0.037	0.16	0.176	0.465	0.914	0.03	0.079	0
85	0.004	0.234	0.176	0.021	0.978	0.646	0.589	0.048	0.224	0.055
86	0	0.745	0.079	0.16	0.808	0.552	0.892	0.016	0.017	0.003
87	0	0.387	0.005	0.358	0.245	0.372	0.957	0.021	0.028	0

8.4. Legend based on the reference library 75 classes (MLC_75C) and CORINE Land Cover 2000 Level 2 classes. Values represents the count of pixels (multiply x 1km^2, to obtain area). Part a.

Class name	11	12	13	14	21	22	23	…
Class 1			1					
Class 13	628	201	129	74	254	2	37	..
Class 15	57	8	2	1	2725	2	328	..
Class 16	759	234	81	85	1842	11	467	..
Class 17	132	16	5	17	1873		166	..
Class 19	308	26	22	15	3816	6	210	..
Class 2		2	21				1	..
Class 20	250	40	18	17	5209	8	253	..
Class 21	133	12	6	3	5145	4	106	..
Class 24	174	9		5	1917	17	1064	..
Class 25	180	76	25	20	450		69	..
Class 26	340	59	21	24	1841	58	490	..
Class 27	84	2	6		2884	2	51	..
Class 28	31	6	1	1	3305	11	120	..
Class 3	58	37	48	1	12		12	..
Class 30	66	2	1	3	4720	2	93	..
Class 32	278	28	7	6	5975	40	777	..
Class 33	47	8		3	4161	3	267	..
Class 34	131	27	4	8	3743	11	217	..
Class 39	164	17	2	8	4622	11	395	..
Class 4	128	4	1	2	4141	6	88	..
Class 41	23	2			2471	6	52	..
Class 42	95	20	2	1	4140	9	313	..
Class 44	14	1	2	2	1537	2	516	..
Class 45	281	9		5	2565	16	314	..
Class 46	72	13	3	2	3231	3	940	..

Class 47	80	11	3	6	3015	11	310	..
Class 48	72	12		11	2032	3	432	..
Class 49	143	3	3	11	2136	74	1944	..
Class 5	498	178	25	95	279	1	71	..
Class 50	205	14	8	8	2528	453	1044	..
Class 51	131	29	12	12	2668	11	1167	..
Class 52	7		1		1		42	..
Class 55	128	1	1	2	593		799	..
Class 56	60	10	9	6	1151	17	638	..
Class 57	43	11		2	2508	2	420	..
Class 59	64	6	1	4	1965	1	1803	..
Class 60	166	35	13	12	1891	4	409	..
Class 61	71		2	1	848	9	219	..
Class 63	7			1	19		74	..
Class 64	19	1	1		915		1899	..
Class 65	6	6	5	2	568	1	223	..
Class 66	80	21	3	24	972	5	1648	..
Class 67	16		1		64		260	..
Class 68	15	14	7	4	1041		328	..
Class 69	23	7		4	874	4	679	..
Class 7								..
Class 70	2				123		113	..
Class 71	38	8			1537	1	270	..
Class 72	10	9	3	3	188		123	..
Class 73	13	5	1		315	1	247	..
Class 74	22	9	1	5	696		912	..
Class 75	7	3		3	157		162	..
Class 76	4				41		44	..
Class 77	25	6	1	3	169	2	190	..
Class 78	2	2		1	19		35	..
Class 79	2	1	1	8	41		49	..
Class 8	47	6	4	1	2477	3	52	..
Class 80	1				4		28	..
Class 81	1			3	101		141	..
Class 82	8			4	99	1	165	..
Class 83	32	8	4		596	1	232	..
Class 84				1	6		40	..
Class 85					3		15	..
Class 86	1				21		28	..
Class 87		1			10		20	..
Class 9	498	112	27	56	1520	5	108	..
MERGED 0611	142	9	1	7	3888	5	410	..

MERGED 1012	272	25	9	9	5954	9	561	..
MERGED 1423	83	3	2	1	4266	2	105	..
MERGED 1822	217	14	3		10217	13	1007	..
MERGED 2937	101	4	4	1	4395	7	344	..
MERGED 4062	103	5	7	4	2071		388	..
MERGED 5458	274	15	12	3	2747	18	630	..
MMERGED 3153	111	11	1	3	2846	2	690	..
Unclassified	1				6		1	..
Total Of COUNT	8284	1474	584	624	143160	896	28865	..

8.5. Legend based on the reference library 75 classes (MLC_75C) and CORINE Land Cover 2000 Level 2 classes. Values represents the count of pixels (multiply x 1km^2, to obtain area). Part b.

Class_name	24	31	32	33	41	51	52	255	Total of counts
Class 1						259	231	1837	2328
Class 13	94	91	53	51	4	76	4	29	1727
Class 15	1237	419	17		20	285		61	5162
Class 16	913	585	64	5	28	194	4	1	5273
Class 17	813	426	3		9	119	1	1	3581
Class 19	419	236	20	2	2	42			5124
Class 2		7	2	48	5	210	57	300	653
Class 20	663	200	7		25	63			6753
Class 21	401	79	1	1	6	43			5940
Class 24	1115	998	13		78	56		451	5897
Class 25	124	487	182	79	3	136	11	32	1874
Class 26	716	485	9	7	8	102		86	4246
Class 27	190	42				3			3264
Class 28	394	142	2		3	43			4059
Class 3	7	30	3	21	11	251	62	140	693
Class 30	186	141			4	32			5250
Class 32	1520	741	13		5	16			9406
Class 33	328	387	4		7	65		14	5294
Class 34	481	487	1			16			5126
Class 39	450	701	11	2	5	49			6437
Class 4	805	238	1		3	2		11	5430
Class 41	96	111				9	1		2771
Class 42	376	585	6		7	84	9	1	5648
Class 44	535	875	56		329	154		254	4277
Class 45	1845	687	5		1	24		182	5934

Class 46	1044	1722	41		7	23			7101
Class 47	249	488	1	3	4	65	14		4260
Class 48	552	1201	11	2	20	153			4501
Class 49	1090	2131	34	1	15	89		104	7778
Class 5	96	87	9	9	40	423	36	70	1917
Class 50	1237	1147	30	7	12	41			6734
Class 51	620	1889	30		20	82			6671
Class 52	15	382	242	3	6	3		5	707
Class 55	590	663	85		13	16		127	3018
Class 56	598	2347	128	2	15	27		9	5017
Class 57	234	905	4		4	13	3		4149
Class 59	730	2101	42	1	42	60		98	6918
Class 60	401	1422	42	21	5	97			4518
Class 61	999	1618	8			15		70	3860
Class 63	122	1370	189		7	1		6	1796
Class 64	450	926	22		24	15			4272
Class 65	213	2785	95	3	7	21			3935
Class 66	304	1143	64	13	79	189	17	2	4564
Class 67	127	2129	98			5		83	2783
Class 68	360	2277	58	2	11	105		10	4232
Class 69	185	1795	12		25	39		1	3648
Class 7		42	169	49		1			261
Class 70	85	1911	24		29	42		213	2542
Class 71	128	1462	17		1	30			3492
Class 72	127	2961	62	24	13	81		2	3606
Class 73	211	2542	98		8	20		131	3592
Class 74	228	2327	36	4	15	49			4304
Class 75	125	2669	40	1	13	153		52	3385
Class 76	65	2527	11			1		81	2774
Class 77	185	3712	232	1	21	37		36	4620
Class 78	25	1875	28		14	12		80	2093
Class 79	50	4087	213		9	4		4	4469
Class 8	317	60	4		1	8			2980
Class 80	11	2147	125		9	2		44	2371
Class 81	44	2645	24	2	12	23		1	2997
Class 82	44	2870	31	1	9	61	1		3294
Class 83	161	3837	209	7	17	68			5172
Class 84	16	3385	31	2	3	22			3506
Class 85	3	2177	24		6	2		29	2259
Class 86	17	2836	48	1	3	25			2980
Class 87	15	4137	111		1	11			4306
Class 9	350	100	14	3	4	108	2	15	2922

MERGED 0611	651	437	6		3	27		225	5811
MERGED 1012	1280	390	12		7	54		32	8614
MERGED 1423	453	125			2	33			5075
MERGED 1822	1656	884	4		24	77		35	14151
MERGED 2937	602	404	6	2	16	26			5912
MERGED 4062	545	1390	43		10	78		373	5017
MERGED 5458	2115	1893	66		2	44			7819
MMERGED 3153	571	738	16		13	24		89	5115
Unclassified		5	1				2	11	27
Total Of COUNT	34004	96283	3423	380	1184	4938	455	5438	329992